

Research Article

Novel Likely Pathogenic Variants Identified by Panel-Based Exome Sequencing in Congenital Cataract Patients

Doudou Chen,^{1,2,3} Tao Yang,⁴ and Siquan Zhu^{1,2,3,5} 

¹Eye School of Chengdu University of Traditional Chinese Medicine, Chengdu 610075, Sichuan, China

²Department of Ophthalmology, Ineye Hospital of Chengdu University of Traditional Chinese Medicine, Chengdu 610032, Sichuan, China

³Key Laboratory of Sichuan Province Ophthalmopathy Prevention and Cure and Visual Function Protection, Chengdu University of Traditional Chinese Medicine, Chengdu 610032, Sichuan, China

⁴Department of Traditional Chinese Medicine, Beijing Tian Tan Hospital, Capital Medical University, Beijing 100050, China

⁵Department of Ophthalmology, Beijing Anzhen Hospital, Capital Medical University, Beijing 100006, China

Correspondence should be addressed to Siquan Zhu; siquan_zhu01@sina.com

Received 30 July 2020; Accepted 2 October 2021; Published 17 November 2021

Academic Editor: Akio Oishi

Copyright © 2021 Doudou Chen et al. This is an open access article distributed under the Creative Commons Attribution License, which permits unrestricted use, distribution, and reproduction in any medium, provided the original work is properly cited.

Purpose. To identify likely pathogenic variants in three families with congenital cataracts via panel-based exome sequencing. **Methods.** A panel containing 153 genes associated with congenital cataracts was designed. Genes were selected through reference to databases including the Human Gene Mutation Database (HGMD), Online Mendelian Inheritance in Man (OMIM), Genetic Home Reference, and the latest peer-reviewed publications on the genetics of hereditary cataracts. Panel-based exome sequencing was performed with the Illumina HiSeq X-Ten platform, and then the identified variants were confirmed with Sanger sequencing and evaluated according to the American College of Medical Genetics and Genomics (ACMG) criteria. **Results.** Three likely pathogenic variants were found. A novel *CRYBB2*: c.230G > T p.G77V variant was identified in family A, a novel *CRYBB2*: c.230G > A p.G77D variant was identified in family B, and a novel *CRYGD*: c.475delG p.A159Pfs*9 variant was identified in family C. **Conclusion.** Panel-based exome sequencing revealed three likely pathogenic variants in three unrelated Chinese families with congenital cataracts. These data expand the genetic spectrum associated with congenital cataracts.

1. Introduction

Autosomal dominant congenital cataracts (ADCCs) are congenital eye abnormalities with phenotypic variability from congenital cataracts, and some but not all lead to early visual impairment. ADCCs may impede visual development by affecting lens transparency and may develop before or after birth. Hereditary factors can account for 10–25% of all congenital cataracts [1]. Congenital cataracts are responsible for 5–20% of blindness in individuals living in developed countries and 22–30% in those living in developing countries [2].

Congenital or developmental cataracts demonstrate significant genotypic and phenotypic variability. Recent studies have identified an increasing number of loci and genes associated with congenital cataracts. Until May 12,

2021, the Online Mendelian Inheritance in Man (OMIM) database included 42 non-syndrome-related genes and 27 syndrome-related genes, including genes encoding α -, β -, and γ -crystallins, such as *CRYAA* (NG_009823.1), *CRYBB2* (NG_009827.1), and *CRYGD* (NG_008039.1); α -connexins, such as *GJA3* (NG_016399.1) and *GJA8* (NG_016242.1); other lens membrane or cytoskeletal proteins genes, such as *MIP* (NG_021397.2) and *BFSP2* (NG_ and 012425.1); several transcription factors, such as *HSF4* (NG_009294.1) and *PITX3* (NG_008147.1); and an expanding group of functionally divergent genes, including *EPHA2* (NG_021396.1), *TDRD7* (NG_028984.1), and *FYCO1* (NG_031955.1) [1, 3–5].

Previously, Sanger sequencing combined with linkage analysis was used to identify the pathogenic genes in

hereditary cataracts. Currently, panel-based targeted exome sequencing is a practical method for identifying monogenic diseases. A specific Hereditary Eye Disease Enrichment Panel developed by MyGenostics (Beijing, China) has been used to identify a variety of genetic eye diseases.

2. Materials and Methods

2.1. Participants. Three Han Chinese families were recruited. One hundred unrelated healthy subjects were also recruited from the physical examination centre. A detailed medical history of the participants was obtained. All participants underwent slit-lamp ophthalmoscopy, biometry, and best-corrected vision acuity (BCVA) as measured with ETDRS linear optotypes/picture symbols. All members of the control group had no anterior segment disease, no fundus disease, no refractive error, no history of trauma, and no family history of genetic disease. The DNA samples were extracted using a DNA Blood Midi Kit (Qiagen, Hilden, Germany). Ethics committee approval was obtained from the Institutional Review Board of Chengdu University of Traditional Chinese (CMEC2010-22), and written informed consent was provided by all participants.

2.2. Targeted Gene Enrichment and Sequencing. One hundred fifty-three genes (Table S1) associated with congenital cataracts were selected via a gene capture strategy using a GenCap custom enrichment kit (MyGenostics, China) following the manufacturer's instructions [6]. The capture probe was designed to cover all exon regions of the target gene without repeating regions. The extracted DNA was eluted and amplified, polymerase chain reaction (PCR) products were purified with SPRI beads (Beckman, USA), and the enriched library was read and sequenced with the Illumina HiSeq X-Ten system.

2.3. Bioinformatics Analysis and Variant Selection. Panel-based targeted exon sequencing (TES) was performed on the probands and their parents. The raw data were saved in FASTQ format. Illumina sequencing adapters and low-quality reads (<80 bp) were filtered by Cutadapt [7]. After quality control, the clean reads were mapped to the UCSC hg38 human reference genome using Burrows–Wheeler Aligner (BWA) [8]. Duplicated reads were removed using Picard tools, and only uniquely mapped reads were used for variation detection. Single-nucleotide polymorphisms (SNPs) and indels were detected by GATK [9]. The variants were further subjected to annotation via ANNOVAR [10], searches in multiple databases, such as 1000 Genomes, ESP6500.exon.program, dbSNP, gnomAD, InterVar, SPI-DEX, REVEL, MCAP, Inhouse (MyGenostics), and Human Gene Mutation Database (HGMD), and prediction analysis via SIFT [11], PolyPhen-2 [12], MutationTaster [13], and GERP++ [14, 15]. The interpretation and evidence grading of the variants were performed according to the latest edition of the standards and guidelines for the interpretation of gene variation issued by the American College for Medical Genetics and Genomics (ACMG) [4, 16–18].

2.4. Validation of Candidate Variants and Segregation. Regions harbouring point variants were amplified. Polymerase chain reaction (PCR) and Sanger sequencing were used to verify putative variants in all participants and controls. Purified PCR products were sequenced using an ABI 3730 Automated Sequencer (PE Biosystems, USA). PCR primers were designed by Invitrogen, Shanghai, China, as follows: *CRYBB2* forward primer (5'-GGCCCCCTCACC-CATACTCA-3') and reverse primer (5'-CTTCCCT-CCTGCCTCAACCTAATC-3'); *CRYGD* forward primer (5'-GCTTTTCTTCTCTTTTATTCTGG-3'), reverse primer (5'-AAGAAAGACACAAGCAAATCAGT-3').

2.5. Bioinformatics Analysis. Pymol shows the protein structure of wild type and variant. Additionally, the potential functional influence from the variant was calculated by PolyPhen-2 and SIFT. Kyte–Doolittle algorithm of ProtScale was adopted to analyze the hydrophobic properties and chemical parameters of protein.

3. Results

The clinical results of the three families are shown in Table 1.

3.1. Family A. The pedigree chart of family A is shown in Figure 1(a). The proband (III.1) presented with bilateral complete cataracts at birth (Figure 1(b)). She underwent binocular cataract surgery sequentially without implantation of an intraocular lens at 2 months. Postoperatively, she was corrected with glasses. She underwent bilateral intraocular lens implants at the age of 2 years. Her BCVA at the age of 4 years was 1.0 logMAR (Snellen equivalent 20/200) in the right eye and 1.0 logMAR (Snellen equivalent 20/200) in the left eye as measured with ETDRS picture symbols. Her anterior segment had no other abnormalities except for cataracts and partial iris loss. This partial iris loss may have been caused by postoperative complications. The fundus cup-to-disc ratio was 0.2 in the right eye and 0.2 in the left eye, and no abnormalities were found in the fundus periphery. She did not have an afferent pupillary defect. Her motility was full, with esotropia. Nystagmus secondary to low vision was present. Her mother (II.1) also presented with bilateral complete cataracts at birth. She underwent bilateral cataract surgery sequentially with intraocular lens implantation at the age of 2 years. There was no refractive correction after the operation. Her BCVA at the age of 32 years was 1.3 logMAR (Snellen equivalent 20/400) in the right eye and 1.0 logMAR (Snellen equivalent 20/200) in the left eye as measured with ETDRS linear optotypes. Except for cataracts, no other abnormalities were found in her anterior segment. She did not have an afferent pupillary defect, but she had esotropia and nystagmus that may have been triggered by low vision. On fundus examination, the binocular cup-to-disc ratio was 0.3, and no abnormalities were found in the fundus periphery. Her grandfather (I.1) also presented with complete bilateral congenital cataracts at birth. He underwent cataract surgery sequentially without intraocular lens implantation at the age of 2 years. There was no refractive

TABLE 1: Clinical information of patients from three families.

| Patient | BCVA (R/L) LogMAR | Type of cataracts | Age of removal of cataract | IOL vs. aphakia | Fundus anomalies | Refractive error at age examined (R/L) | Nystagmus | Strabismus subtype | |
|----------|-------------------|-------------------|-----------------------------|-----------------|------------------|--|--|----------------------|-----------|
| Family A | III.1 | 1.0/1.0 | Bilateral complete cataract | 2 months | IOL | No | +6.00DS/-2.00DC×10, +5.50DS/-1.00DC×140 | Ophthalmic nystagmus | Esotropia |
| | II.1 | 1.3/1.0 | Bilateral complete cataract | 2 years | IOL | No | +1.00DS/-0.50DC×60, -2.250DS/-1.00DC×80 | Ophthalmic nystagmus | Esotropia |
| | I.1 | 1.7/1.6 | Bilateral complete cataract | 2 years | aphakia | Optic atrophy | +19.00DS/-0.50DC×60, +22.50DS/-1.50DC×30 | Ophthalmic nystagmus | Esotropia |
| Family B | III.1 | 1.0/0.7 | Bilateral nuclear cataract | 2 months | IOL | No | NA | No | No |
| | II.1 | 0.4/0.7 | Bilateral nuclear cataract | 2 years | IOL | No | +2.00DS/-1.50DC×170, +1.50DS/-1.50DC×110 | No | No |
| | I.1 | 0.7/1.0 | Bilateral nuclear cataract | 4 years | IOL | No | +5.00DS/-1.75DC×50, +5.50DS/-1.00DC×110 | No | No |
| Family C | III.3 | 1.0/1.0 | Bilateral nuclear cataract | 3 years | IOL | No | +4.50DS/-1.00DC×5, +6.00DS/-2.00DC×160 | Ophthalmic nystagmus | Esotropia |
| | II.2 | 0.5/0.4 | Bilateral nuclear cataract | 5 years | IOL | No | +1.25DS/-0.75DC×130, +2.00DS/-1.50DC×90 | Ophthalmic nystagmus | Esotropia |
| | I.2 | 1.7/1.6 | Bilateral nuclear cataract | 6 years | aphakia | No | +17.00DS/-2.00DC×95, +18.50DS/-1.00DC×60 | Ophthalmic nystagmus | Esotropia |
| | II.1 | 0.7/1.0 | Bilateral nuclear cataract | 4 years | IOL | No | -0.50DS/-1.50DC×30, +1.50DS/-2.00DC×70 | No | No |
| | III.1 | 1.0/1.0 | Bilateral nuclear cataract | 4 years | IOL | No | +1.75DS/-0.75DC×180, +2.00DS/-1.75DC×90 | No | No |

BCVA: best-corrected visual acuity. The best-corrected visual acuity was measured and calculated with the EDTRS visual acuity chart and represented with logMAR. Snellen equivalent is shown in the text. Bilateral nuclear cataract in family B has more opacity in the lens nucleus, while bilateral nuclear cataract in family A has less opacity. IOL: intraocular lens. NA: not acquired. NO: not found; R: right; L: left.

correction after the surgery. His BCVA at the age of 55 years was 1.7 logMAR (Snellen equivalent 20/1000) in the right eye and 1.6 logMAR (Snellen equivalent 20/800) in the left eye as measured with ETDRS linear optotypes. Except for irregular pupils that may have been caused by surgical complications, there were no other abnormalities. He did have an afferent pupillary defect that may have been associated with partial atrophy of the optic nerve. He also had esotropia and nystagmus secondary to low vision. On fundus examination, the binocular cup-to-disk ratio was 0.4, and the optic disc was pale. Optical coherent fundus examination revealed that the optic disc nerve fibre layer was thin with some optic nerve atrophy. However, the intraocular pressure was within the normal range.

3.2. Family B. The pedigree chart of family B is shown in Figure 2(a). The proband (III.1) presented with bilateral nuclear cataracts at the age of 2 months (Figure 2(b)), and she underwent bilateral cataract surgery sequentially with

intraocular lens implantation at the age of 2 years. After the operation, she was corrected with glasses. Her BCVA at the age of 2 years was 1.0 logMAR (Snellen equivalent 20/200) in the right eye and 0.7 logMAR (Snellen equivalent 20/100) in the left eye as measured with ETDRS picture symbols. Her anterior segment was normal except for cataracts. She did not have an afferent pupillary defect, and the cup-to-disk ratio of both eyes was 0.3 on fundus examination. Her motility was full, without strabismus and nystagmus. Her father (II.1) was found to squint frequently at the age of 2 years. He was diagnosed with binocular nuclear cataracts and underwent sequential bilateral cataract surgery combined with intraocular lens implantation. His BCVA at the age of 30 years was 0.4 logMAR (Snellen equivalent 20/50) in the right eye and 0.7 logMAR (Snellen equivalent 20/100) in the left eye as measured with ETDRS linear optotypes. His anterior segment had no other abnormalities except for cataracts. Fundus examination of the binocular cup-to-disk ratio was 0.2, and there were no other abnormalities. He did not have an afferent pupillary defect. His motility was full.

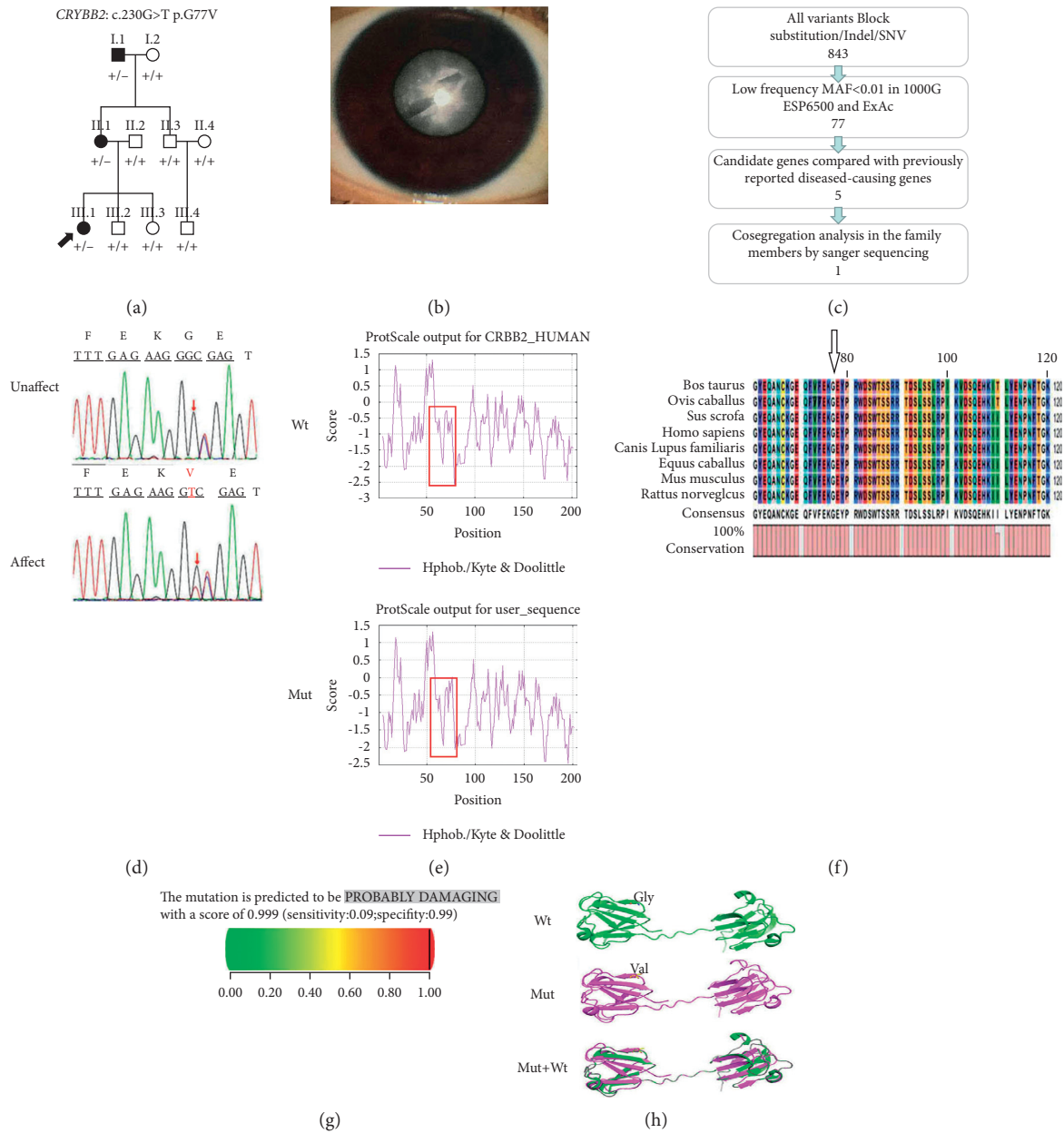


FIGURE 1: (a) Pedigree of ADCC family A Squares and circles indicate males and females, respectively. The solid black arrow indicates the proband (III.1). (b) A photograph of the proband's (III.1) lens is shown. (c) Schematic representation of the filter strategies employed in our study. (d) Sanger sequencing results. (e) Hydropathic characteristics caused by changes in the variant protein. (f) Multiple protein sequence alignment. (g) The score obtained from PolyPhen-2 analysis was 0.999. (h) The structures of the homomeric WT and variant *CRYBB2* c.230G > T; p.G77V proteins were modelled in PyMOL.

The grandmother did not have any abnormalities at birth, but her family discovered that she had poor vision in both eyes at the age of 4 years. The grandmother (I.2) also presented with binocular nuclear cataracts. She underwent sequential bilateral cataract surgery with intraocular lens implantation at the age of 4 years. Her BCVA at the age of 55 years was 0.7 logMAR (Snellen equivalent 20/100) in the right eye and 1.0 logMAR (Snellen equivalent 20/200) in the left eye as measured with ETDRS linear optotypes. Her anterior segment had no other abnormalities except for cataracts. Fundus examination revealed a cup-to-disk ratio

of 0.2 for both eyes and no other abnormalities. She did not have an afferent pupillary defect. Her motility was full, without strabismus and nystagmus.

3.3. *Family C*. The pedigree chart of family C is shown in Figure 3(a). The proband (III.3) gradually presented with binocular nuclear cataracts within one year after birth (Figure 3(b)). He underwent sequential binocular cataract surgery at the age of 3 years. After the operation, he did not undergo any vision correction procedure. His BCVA at the

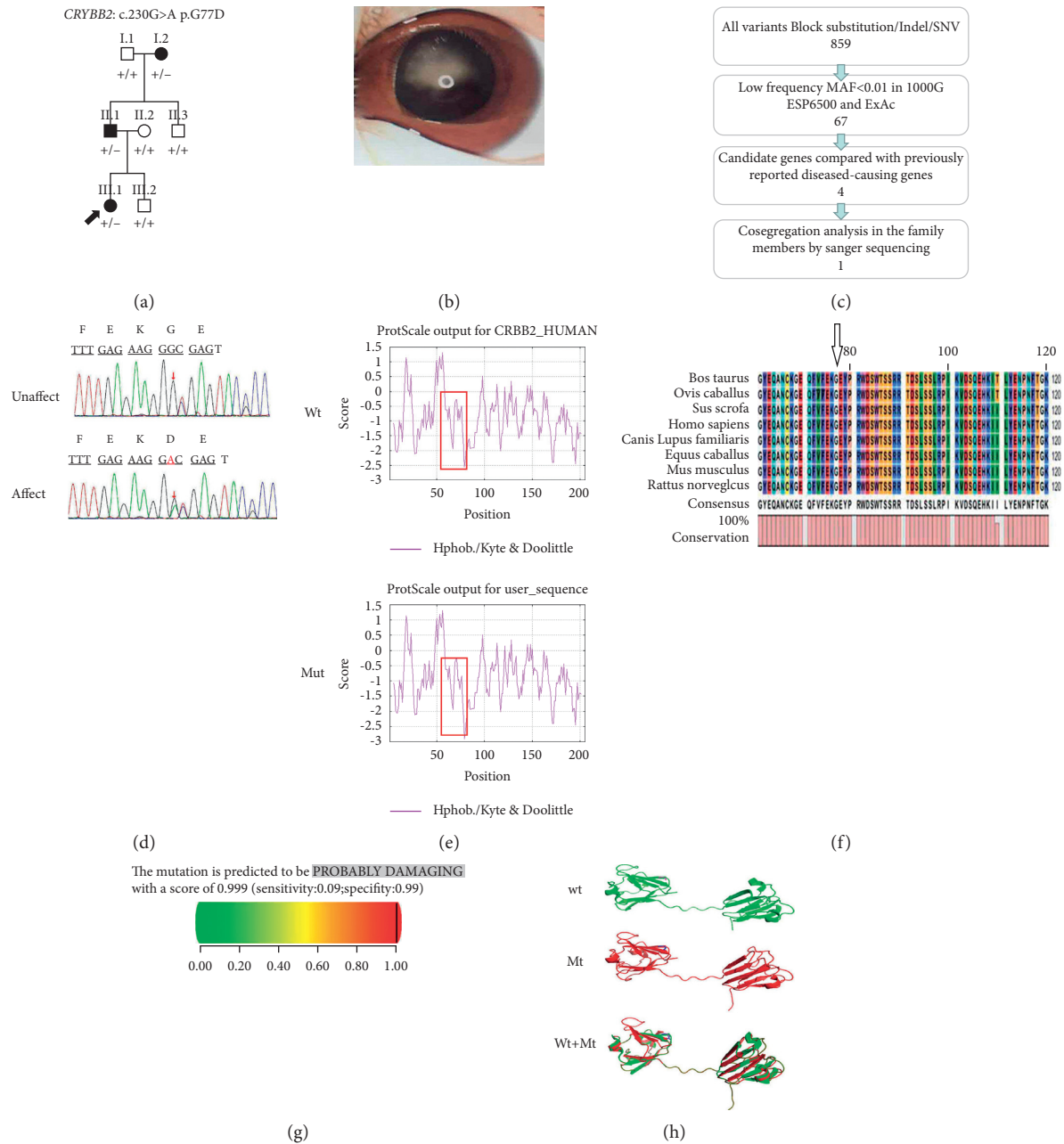


FIGURE 2: (a) Pedigree of ADCC family B The solid black arrow indicates the proband (III.1). (b) A photograph of the proband's (III.1) lens is shown. (c) Schematic representation of the filter strategies employed in our study. (d) Sanger sequencing results. (e) hydropathic characteristics caused by changes in the variant protein. (f) Multiple protein sequence alignment. (g) The score obtained from PolyPhen-2 analysis was 0.999. (h) The structures of the homomeric WT and variant *CRYBB2*: c.230G > A; p.G77D proteins were modelled in PyMOL.

age of 3 years was 1.0 logMAR (Snellen equivalent 20/200) in the right eye and 1.0 logMAR (Snellen equivalent 20/200) in the left eye as measured with ETDRS picture symbols. His anterior segment had no abnormalities except for cataracts. Fundus examination revealed that the cup-to-disk ratio of both eyes was 0.3, and he did not have an afferent pupillary defect. His motility was full, with esotropia. Nystagmus secondary to low vision was noted. His father (II.2) gradually developed binocular nuclear cataracts within five years after birth, and he underwent sequential binocular cataract surgery at the age of 5 years. After the operation, he did not

undergo any vision correction procedure. His BCVA at the age of 30 years was 0.5 logMAR (Snellen equivalent 20/63) in the right eye and 0.4 logMAR (Snellen equivalent 20/50) in the left eye as measured with ETDRS linear optotypes. His anterior segment had no other abnormalities except for cataracts. Fundus examination revealed that the cup-to-disk ratio of both eyes was 0.2. His mobility was full, and he did not have an afferent pupillary defect. He also had mild esotropia and nystagmus that may have been secondary to low vision. The grandmother (I.2) also presented with bilateral nuclear cataracts at the age of 2 years and underwent

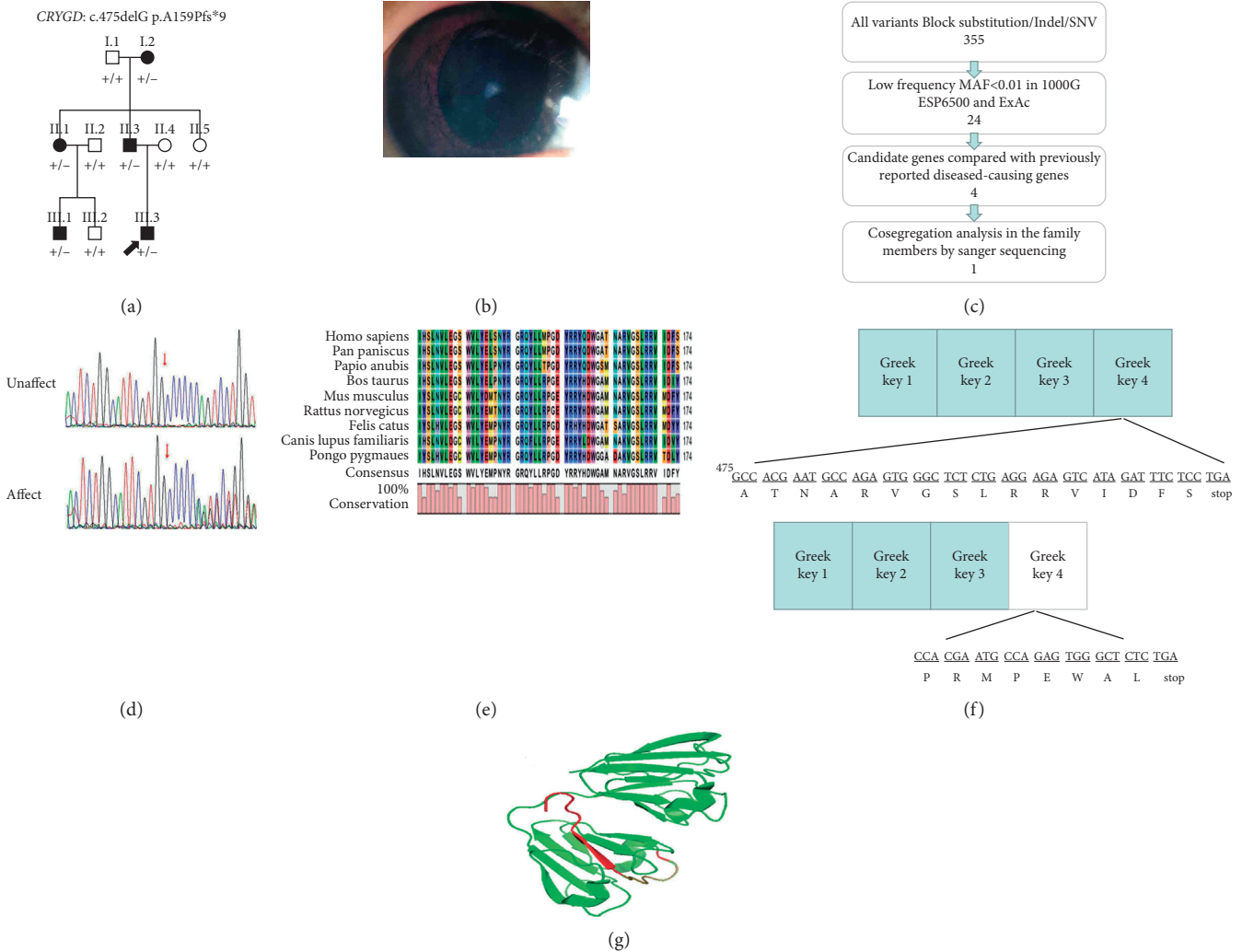


FIGURE 3: (a) Pedigree of ADCC family C The solid black arrow indicates the proband (III.3). (b) Photographs of the proband's (III.3) lens are shown. (c) Schematic representation of the filter strategies employed in our study. (d) Sanger sequencing results. (e) Multiple protein sequence alignment. (f) The identified variant, *CRYGD*: c.475delG; p.A159Pfs*9, generated a frameshift and premature termination from a position 9 codons downstream (p.A159Pfs*9) of the variant; these alterations resulted in a protein that was reduced to half the length of the full-length protein. (g) The structures of the *CRYGD* proteins were modelled in PyMOL.

cataract extraction without intraocular lens implantation. Her BCVA at the age of 65 years was 1.7 logMAR (Snellen equivalent 20/900) in the right eye and 1.6 logMAR (Snellen equivalent 20/800) in the left eye as measured with ETDRS linear optotypes. Her anterior segment had no other abnormalities except for cataracts. Fundus examination revealed that the cup-to-disk ratio of both eyes was 0.2. Additionally, she had esotropia with nystagmus that may have been secondary to low vision. Another family member (II.1) was also diagnosed with congenital cataracts and underwent cataract surgery at the age of 4 years. Her BCVA at the age of 33 years was 0.7 logMAR (Snellen equivalent 20/100) in the right eye and 1.0 logMAR (Snellen equivalent 20/200) in the left eye as measured with ETDRS linear optotypes. Fundus examination revealed that the binocular cup-to-disk ratio was 0.2, without strabismus or nystagmus, and pupil defects. Another family member (III.1) was also diagnosed with congenital cataracts and underwent cataract

surgery at the age of 4 years. His BCVA at the age of 11 years was 1.0 logMAR (Snellen equivalent 20/200) in the right eye and 1.0 logMAR (Snellen equivalent 20/200) in the left eye as measured with ETDRS linear optotypes. However, except for cataracts, he had no other abnormalities in the anterior segment, no strabismus or nystagmus, no pupil defects, and had a cup-to-disk ratio of 0.2 (fundus examination).

3.4. Sequencing Results and Biological Analysis. Sequencing results and biological analysis are described in the supplementary materials (available here), and sequencing data statistics are shown in Table 2. The predictive analysis of variant function is presented in Table 3, and candidate variants are shown in Table S2. The sequencing chromatograms of the three family members are shown in supplementary outcomes 1 (Sanger A, Sanger B, and Sanger C) and the sequencing biological analysis results of the three families are shown in supplementary outcomes 2.

TABLE 2: Summary of probands sequencing data in three families.

| Samples | Proband (family A) | Proband (family B) | Proband (family C) |
|--|--------------------|--------------------|--------------------|
| Raw_data_bases (Mb) | 2726.51 | 2825.35 | 1443.22 |
| Clean_data_bases (Mb) | 2615.89 | 2630.75 | 1393.44 |
| Aligned_bases (Mb) | 2597.73 | 2618.71 | 1387.15 |
| Aligned (%) | 99.31 | 99.54 | 99.55 |
| Initial bases on target | 456294 | 456294 | 455256 |
| Base covered on target | 453517 | 453355 | 451520 |
| Coverage of target region (%) | 99.39 | 99.36 | 99.18 |
| Effective bases on target | 177513627 | 189678089 | 127259738 |
| Fraction of effective bases on target (%) | 6.83 | 7.24 | 9.17 |
| Average sequencing depth on target | 389.03 | 415.69 | 279.53 |
| Fraction of target covered with at least 4X (%) | 99.16 | 99.09 | 98.73 |
| Fraction of target covered with at least 10X (%) | 98.95 | 98.78 | 97.89 |
| Fraction of target covered with at least 20X (%) | 98.28 | 98.01 | 95.63 |
| Duplication rate (%) | 22.72 | 24.99 | 28.34 |

TABLE 3: Summary of function prediction of three likely pathogenic variants.

| Gene symbol | CRYBB2 (family A) | CRYBB2 (family B) | CRYGD (family C) |
|--|-------------------|-------------------|--------------------------|
| ID | chr22-25623876 | chr22-25623876 | chr2-208986446 208986447 |
| Ref_Transcript | NM_000496 | NM_000496 | NM_006891 |
| Exon | exon4 | exon4 | exon3 |
| Nucleotide_Changes | c.230G>T | c.230G>A | c.475delG |
| Amino_Acid_Changes | p.G77V | p.G77D | p.A159Pfs*9 |
| Gene_Type | het | het | het |
| Pathogenic_Analysis | Uncertain | Uncertain | Likely pathogenic |
| clinvar | — | — | — |
| MutRatio | 0.39 | 0.45 | 0.55 |
| Mutation_Type | SNV | SNV | deletion |
| dbSNP | — | — | — |
| PathSNP | #N/A | #N/A | #N/A |
| MutInNormal | #N/A | #N/A | #N/A |
| 1000Genome | #N/A | #N/A | #N/A |
| MutInDatabase | #N/A | #N/A | #N/A |
| 1000g2015aug_all | — | — | — |
| ESP6500si | — | — | — |
| Inhouse | — | — | — |
| gnomAD_exome_ALL | — | — | — |
| gnomAD_exome_EAS | — | — | — |
| SIFT | 0 | 0 | — |
| SIFT_Predict | Damaging | Damaging | — |
| PolyPhen_2 | 0.999 | 0.999 | — |
| PolyPhen_2_Predict | Probably_damaging | Probably_damaging | — |
| MutationTaster | 1 | 1 | — |
| MutationTaster_Predict | Disease_causing | Disease_causing | — |
| GERP++ | 5.08 | 5.08 | — |
| GERP++_Predict | Conserved | Conserved | — |
| SPIDEX | 0.5789 | 1.3267 | — |
| REVEL_score | 0.957 | 0.968 | — |
| MCAP_score | 0.157318302 | 0.219654258 | — |
| MCAP_pred | P | P | — |
| InterVar | Likely pathogenic | Likely pathogenic | Uncertain_significance |
| Highest-MAF | — | — | — |
| Mygeno_InterACMG | PM2; PP3 | PM2; PP3 | PVS; PM2 |
| Pathogenic_Analysis (based on ACMG guidelines) | Uncertain | Uncertain | Likely pathogenic |

"#N/A" indicates that it does not exist in the database, and "-" indicates the frequency in the database. SIFT predictive value, the smaller the value, the more likely it is to cause disease. PolyPhen prediction value, the larger the value, the more likely it is to cause disease. MutationTaster prediction result, the larger the value, the more likely it is to cause disease. GERP++ indicates the value of predicting conservativeness among various species, and >2 indicates relatively conservative.

4. Discussion

In this study, we used panel-based targeted exome sequencing to identify three novel likely pathogenic variants in three unrelated Chinese families with congenital cataracts. The panel was designed based on a consensus of experts on the genetic diagnosis of eye diseases in July 2018 and by referring to the OMIM database, HGMD, and clinical data. To date, 356 genes associated with syndromic and non-syndromic cataracts and nearly 50 disease-causing genes that are related to isolated cataracts have been identified (<http://cat-map.wustl.edu/>). The pathogenicity of these variant sites was analysed strictly following the ACMG guidelines [17].

CRYBB2:c.230G > T(p.G77V) caused family A to acquire complete cataracts. *CRYBB2*:c.230G > A(p.G77D) caused family B to acquire irregular nuclear cataracts. The p.G77V variant slightly increases hydrophobicity and has a mild effect on the protein structure. In addition, the variant alters a tyrosine corner, which is critical for the stability of the N-terminal domain and may lead to changes in the intermolecular action, solubility and stability of *CRYBB2*. The p.G77D variant causes the hydrophobicity of the variant protein to be lower than that of the wild-type protein and immense changes in charge and size that may also affect the protein's correct folding and stability. There are many intermolecular contacts between domains in *CRYBB2*. Both of these variants may disrupt the dimerization of the *CRYBB2* protein or inhibit its binding to other lens-soluble proteins. These changes may destroy the microstructure of the lens, increase light scattering, and eventually cause the lens to become opaque. *CRYBB2* contains six exons, with the start of translation beginning in the second exon. Exons 3 to 6 each encode one Greek key motif (GKM). The variants in these two families are located in exon 4, which may cause the destruction of the corresponding GKM. At present, a total of 47 *CRYBB2* variants have been reported, 27 of which are unique. The p.W151C variant disrupts the solubility of β B2-crystallin and causes abnormal aggregation of the protein to form membrane cataracts [19]. The p.Q155X variant causes a partially unfolded structure and decreased structural order, inhibiting interactions with other proteins [20]. The p.A188H variant impairs the dimerization of the *CRYBB2* protein by establishing a new hydrogen bond, thereby leading to lens opacity [21]. The p.D128V variant changes the hydrophobicity and charge of the random coil region between amino acids 126–139 of the *CRYBB2* protein [22]. The p.W151C variant identified in an Indian family was predicted to disrupt the fourth GKM and increase the protein's hydrophobicity, thereby leading to the formation of cataracts [23]. Congenital cataracts have complex genetic and clinical heterogeneity [19]. The variants in these two families may be a susceptible mutation site, but further verification is needed.

Patients in family C developed bilateral nuclear cataracts within 1 to 5 years after birth. The identified variant, c.475delG located in the last exon of *CRYGD*, generated by a frameshift variant located 9 codons downstream that resulted in premature termination (p.A159Pfs*9), resulted in a protein that was reduced to half the length of the full-length protein. In eukaryotes, mRNAs that contain

premature stop codons can be detected and destroyed by an mRNA monitoring mechanism called nonsense-mediated decay (NMD). However, it usually occurs only when the nonsense codon is more than 50 nucleotides upstream of the last exon junction [24, 25]. Due to the variant p.A159Pfs*9 is located at the end of the last exon in *CRYGD*, it should escape from NMD, resulting in translation of the truncated protein. In addition, the *CRYGD* gene contains four GKMs, each of which is approximately forty amino acids long. Two similar GFM motifs form a structural domain, resulting in a total of two structural domains. The specificity of domain interface interactions is likely important for preventing incorrect associations in the lens' nucleus due to high protein concentrations. We speculate that the p.A159Pfs*9 in family C removes the last beta strand of the fourth GKM, destabilizing the fourth GKM severely and hence the entire domain. This protein probably does not fold normally, even during synthesis. This would destabilize the protein severely by eliminating a required part of the fourth GKM, which would bind to alpha-crystallin until it is overwhelmed and then either become toxic to the lens cell or form aggregates large enough to scatter light. A polypeptide or protein with a complete primary structure can function only if folded correctly to form the correct spatial structure. Changes in protein properties caused by variants may affect their functions and interactions with other proteins, leading to cataracts. Approximately 59 *CRYGD* variants have been documented to be associated with congenital cataracts, 25 of which are unique, and the remainder are recurrent. Most of these reported variants are single-base variants. p.G165fs is the only frameshift variant that has been previously reported [26]. In this research, the *CRYGD*: p.A159Pfs*9 we discovered in this family C is a novel frameshift variant. However, there is no report on the monomerization and metabolic activities of gamma-crystallins. There is also a need to explore animal models to elucidate the underlying molecular mechanism by which *CRYBB2* and *CRYGD* variants contribute to cataracts.

5. Conclusions

In this study, we identified three novel likely pathogenic variants, *CRYBB2*: c.230G > T (p.G77V), *CRYBB2*: c.230G > A (p.G77D), and *CRYGD*: c.475delG (p.A159Pfs*9), in three unrelated Chinese families with hereditary cataracts. These data expand the genetic spectrum associated with congenital cataracts. The use of panel sequencing may provide a basis for the genetic diagnosis of congenital cataracts in patients with a family history and meet patients' needs through genetic counselling.

Data Availability

The data used to support the findings of this study are included within the article.

Conflicts of Interest

The authors declare that they have no conflicts of interest.

Authors' Contributions

Dou dou Chen, Tao Yang, and Si quan Zhu designed the study; Si quan Zhu conducted the study; Dou dou Chen and Tao Yang are responsible for the collection and management of the data; Dou Chen, Tao Yang, and Si quan Zhu analysed and interpreted the data; Dou dou Chen and Tao Yang prepared and reviewed the manuscript. All authors gave final approval of the manuscript.

Acknowledgments

The authors are grateful for the cooperation of the involved families. The National Natural Science Foundation of China (no. 51573101), Beijing Natural Science Foundation (no. 7172056), and Xinglin Scholar Scientific Research Promotion Program of Chengdu University of Traditional Chinese Medicine (no. BSH2019025).

Supplementary Materials

Table S1 presents the 153 genes contained in the panel. Table S2 presents the evaluation of candidate variants for each family in silico analysis. The sequencing chromatograms of the three family members are shown in supplementary result 1, and the sequencing biological analysis results of the three families are shown in supplementary result 2. (*Supplementary Materials*)

References

- [1] O. Messina-Baas and S. A. Cuevas-Covarrubias, "Inherited congenital cataract: a guide to suspect the genetic etiology in the cataract genesis," *Molecular syndromology*, vol. 8, no. 2, pp. 58–78, 2017.
- [2] Y.-C. Liu, M. Wilkins, T. Kim, B. Malyugin, and J. S. Mehta, "Cataracts," *The Lancet*, vol. 390, no. 10094, pp. 600–612, 2017.
- [3] A. A. Trumler, "Evaluation of pediatric cataracts and systemic disorders," *Current Opinion in Ophthalmology*, vol. 22, no. 5, pp. 365–379, 2011.
- [4] Y. Yao, X. Zheng, X. Ge et al., "Identification of a novel GJA3 mutation in a large Chinese family with congenital cataract using targeted exome sequencing," *PLoS One*, vol. 12, no. 9, Article ID e0184440, 2017.
- [5] M. Riera, A. Wert, I. Nieto, and E. Pomares, "Panel-based whole exome sequencing identifies novel mutations in microphthalmia and anophthalmia patients showing complex Mendelian inheritance patterns," *Molecular Genetics and Genomic Medicine*, vol. 5, no. 6, pp. 709–719, 2017.
- [6] R. Gao, Y. Liu, A. P. Gjesing et al., "Evaluation of a target region capture sequencing platform using monogenic diabetes as a study-model," *BMC Genetics*, vol. 15, no. 1, p. 13, 2014.
- [7] M. Martin, "Cutadapt removes adapter sequences from high-throughput sequencing reads," *Embnet Journal*, vol. 17, no. 1, 2011.
- [8] H. Li and R. Durbin, "Fast and accurate short read alignment with Burrows-Wheeler transform," *Bioinformatics*, vol. 25, no. 14, pp. 1754–1760, 2009.
- [9] G. A. Van der Auwera, M. O. Carneiro, and C. Hartl, "From FastQ data to high confidence variant calls: the Genome Analysis Toolkit best practices pipeline," *Current protocols in bioinformatics*, vol. 43, no. 1110, pp. 11.10.1–11.10.33, 2013.
- [10] K. Wang, M. Li, and H. Hakonarson, "ANNOVAR: functional annotation of genetic variants from high-throughput sequencing data," *Nucleic Acids Research*, vol. 38, no. 16, p. e164, 2010.
- [11] P. Kumar, S. Henikoff, and P. C. Ng, "Predicting the effects of coding non-synonymous variants on protein function using the SIFT algorithm," *Nature Protocols*, vol. 4, no. 7, pp. 1073–1081, 2009.
- [12] I. A. Adzhubei, S. Schmidt, L. Peshkin et al., "A method and server for predicting damaging missense mutations," *Nature Methods*, vol. 7, no. 4, pp. 248–249, 2010.
- [13] J. M. Schwarz, D. N. Cooper, M. Schuelke, and D. Seelow, "MutationTaster2: mutation prediction for the deep-sequencing age," *Nature Methods*, vol. 11, no. 4, pp. 361–362, 2014.
- [14] G. M. Cooper, E. A. Stone, G. Asimenos, E. D. Green, S. Batzoglou, and A. Sidow, "Distribution and intensity of constraint in mammalian genomic sequence," *Genome Research*, vol. 15, no. 7, pp. 901–913, 2005.
- [15] E. V. Davydov, D. L. Goode, M. Sirota, G. M. Cooper, A. Sidow, and S. Batzoglou, "Identifying a high fraction of the human genome to be under selective constraint using GERP++," *PLoS Computational Biology*, vol. 6, no. 12, Article ID e1001025, 2010.
- [16] ACMG Board of Directors, "ACMG policy statement: updated recommendations regarding analysis and reporting of secondary findings in clinical genome-scale sequencing," *Genetics in Medicine*, vol. 17, no. 1, pp. 68–69, 2015.
- [17] S. Richards, N. Aziz, S. Bale et al., "Standards and guidelines for the interpretation of sequence variants: a joint consensus recommendation of the American College of medical genetics and Genomics and the association for molecular pathology," *Genetics in Medicine*, vol. 17, no. 5, pp. 405–423, 2015.
- [18] R. C. Green, J. S. Berg, W. W. Grody et al., "ACMG recommendations for reporting of incidental findings in clinical exome and genome sequencing," *Genetics in Medicine*, vol. 15, no. 7, pp. 565–574, 2013.
- [19] W. J. Zhao, J. Xu, X. J. Chen, H. H. Liu, K. Yao, and Y. B. Yan, "Effects of cataract-causing mutations W59C and W151C on β B2-crystallin structure, stability and folding," *International Journal of Biological Macromolecules*, vol. 109, no. 5, pp. 100–112, 2017.
- [20] F. F. Li, S. Q. Zhu, S. Z. Wang et al., "Nonsense mutation in the CRYBB2 gene causing autosomal dominant progressive polymorphic congenital coronary cataracts," *Molecular Vision*, vol. 14, no. 90, pp. 750–755, 2008.
- [21] N. Weisschuh, S. Aisenbrey, B. Wissinger, and A. Riess, "Identification of a novel CRYBB2 missense mutation causing congenital autosomal dominant cataract," *Molecular Vision*, vol. 18, no. 20, pp. 174–180, 2012.
- [22] S. Pauli, T. Söker, N. Klopp, T. Illig, W. Engel, and J. Graw, "Mutation analysis in a German family identified a new cataract-causing allele in the CRYBB2 gene," *Molecular Vision*, vol. 13, pp. 962–967, 2007.
- [23] S. T. Santhiya, S. M. Manisastri, D. Rawley et al., "Mutation analysis of congenital cataracts in Indian families: identification of SNPs and a new causative allele inCRYBB2Gene," *Investigative Ophthalmology and Visual Science*, vol. 45, no. 10, pp. 3599–3607, 2004.
- [24] E. Wagner and J. Lykke-Andersen, "mRNA surveillance: the perfect persist," *Journal of Cell Science*, vol. 115, no. 15, pp. 3033–3038, 2002.

- [25] M. Wilkinson, "A new function for nonsense-mediated mRNA-decay factors," *Trends in Genetics*, vol. 21, no. 3, pp. 143–148, 2005.
- [26] L. Y. Zhang, G. H. Yam, D. S. Fan, P. O. Tam, D. S. Lam, and C. P. Pang, "A novel deletion variant of gammaD-crystallin responsible for congenital nuclear cataract," *Molecular Vision*, vol. 13, pp. 2096–2104, 2007.